Electronic Structure and Nesting-Driven Enhancement of the RKKY Interaction at the Magnetic Ordering Propagation Vector in Gd_2PdSi_3 and Tb_2PdSi_3

D. S. Inosov,[1,2] D. V. Evtushinsky,[1] A. Koitzsch,[1] V. B. Zabolotnyy,[1] S. V. Borisenko,[1] A. A. Kordyuk,[1,3] M. Frontzek,[4] M. Loewenhaupt,[4] W. Löser,[1] I. Mazilu,[1] H. Bitterlich,[1] G. Behr,[1] J.-U. Hoffmann,[5] R. Follath,[6] and B. Büchner[1]

[1]*Leibniz Institut für Festkörper- und Werkstoffforschung Dresden, D-01171 Dresden, Germany*
[2]*Max-Planck-Institute for Solid State Research, Heisenbergstraße 1, D-70569 Stuttgart, Germany*
[3]*Institute of Metal Physics of National Academy of Sciences of Ukraine, 03142 Kyiv, Ukraine*
[4]*Institut für Festkörperphysik, Technische Universität Dresden, D-01062 Dresden, Germany*
[5]*Helmholtz-Zentrum Berlin für Materialien und Energie GmbH, D-14109 Berlin, Germany*
[6]*BESSY GmbH, Albert-Einstein-Strasse 15, 12489 Berlin, Germany*

(Received 21 August 2008; published 26 January 2009)

Measurements of the low-energy electronic structure in Gd_2PdSi_3 and Tb_2PdSi_3 by means of angle-resolved photoelectron spectroscopy reveal a Fermi surface consisting of an electron barrel at the Γ point surrounded by spindle-shaped electron pockets originating from the same band. The calculated momentum-dependent RKKY coupling strength is peaked at the $\frac{1}{2}\Gamma K$ wave vector, which coincides with the propagation vector of the low-temperature in-plane magnetic order observed by neutron diffraction, thereby demonstrating the decisive role of the Fermi surface geometry in explaining the complex magnetic ground state of ternary rare earth silicides.

DOI: 10.1103/PhysRevLett.102.046401 PACS numbers: 71.20.Lp, 71.18.+y, 71.27.+a, 79.60.−i

Ternary rare earth silicides with a hexagonal crystal structure of the form R_2PdSi_3, where R is a rare earth atom, are known to exhibit complex magnetic behavior [1–14] due to a delicate competition of the indirect exchange coupling mediated by the conductance electrons, generally known as Ruderman-Kittel-Kasuya-Yosida (RKKY) interaction [15], and the Kondo effect, which are comparable in magnitude [1,2]. Such interplay determines many unusual magnetic, thermal and transport properties, which have stimulated unceasing interest in these materials during the last two decades and are still not fully understood: large negative magnetoresistance [3], quasi-low-dimensional magnetism and spin-glass-like behavior [7,8], highly anisotropic ac susceptibility [7], magnetocaloric effect [9], thermoelectric power [1], and Hall coefficient [1].

Most of the R_2PdSi_3 compounds order magnetically at low temperatures, somewhat below the Kondo minimum in the resistivity [2–6]. The exact type of such ordering strongly depends on the material and can be rather complicated [6,10]. The corresponding Néel temperature T_N reaches maximum for the Gd ($T_N = 21.0$ K [11]) and Tb ($T_N = 23.6$ K [12]) compounds, which we have chosen as the subject of the present study. The RKKY exchange interaction that essentially determines their magnetic properties is mediated by the conductance electrons, and therefore any reasonable description of the corresponding physics is impossible without the knowledge of the Fermi surface and the low-energy electronic structure. According to our recent study [16], the sign reversal of the Hall effect observed at low temperatures in R_2PdSi_3 [13] might be an indication of the opening of the pseudogap at some portions of the Fermi surface, as was also suggested earlier by resistivity measurements [2], again emphasizing the importance of studying the electronic structure of these materials. Nevertheless, though the single crystals of Gd_2PdSi_3 have been available for nearly a decade [3], the fermiology and the underlying electron dispersions are still not known for any of the R_2PdSi_3 compounds neither from momentum-resolved measurements nor from band structure calculations. Earlier photoemission experiments [17,18] were performed only on polycrystalline samples and could not therefore shed light on the dispersion of conductance electrons and the Fermi surface geometry, but have revealed that the density of states at the Fermi level is likely to be dominated by the $5d$ states of the rare earth atoms.

Here we report an angle-resolved photoelectron spectroscopy (ARPES) investigation of the low-energy electronic structure performed on the single crystals of Gd_2PdSi_3 and Tb_2PdSi_3, whose crystal structure is illustrated by Fig. 1. We show that the Fermi surface in both compounds has a flowerlike shape with the dominant nesting vector that coincides with the propagation vector of the

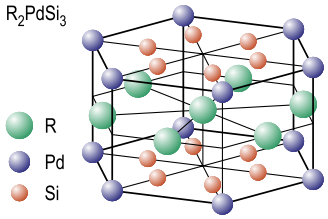

FIG. 1 (color online). Crystal structure of R_2PdSi_3 after Refs. [7,17].

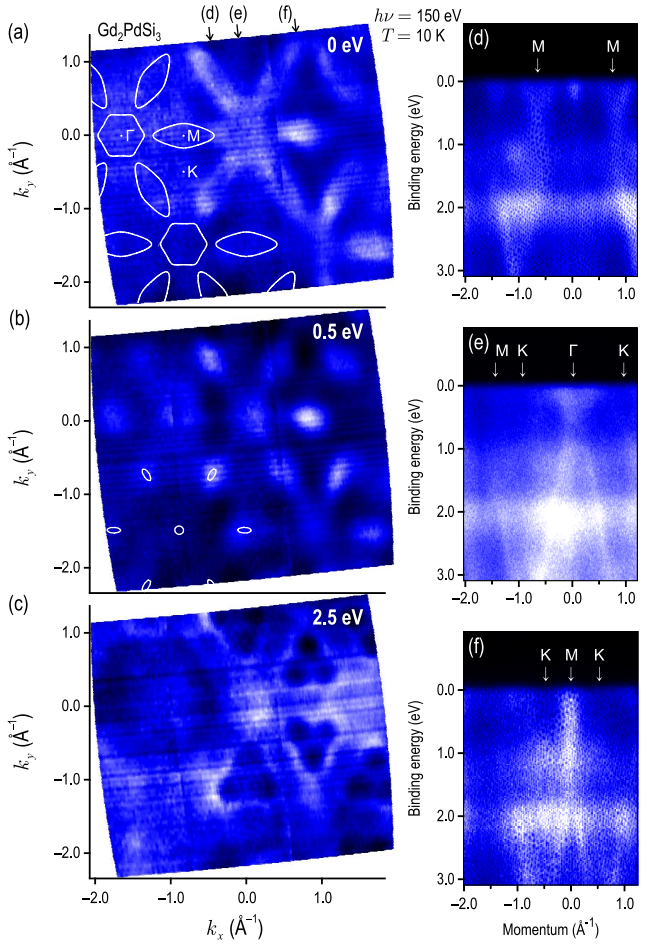

FIG. 2 (color online). Fermi surface and the underlying electronic structure of Gd_2PdSi_3. Lighter colors represent higher photoemission intensity. Panels (a)–(c) show constant energy cuts taken at the Fermi level, at 0.5 and 2.5 eV binding energy, respectively. Panels (d)–(f) show energy-momentum cuts as indicated by arrows in panel (a). The solid white contours in panels (a) and (b) represent the tight-binding fit to the data.

low-temperature magnetic ordering, as we will see from the comparison of our ARPES data and neutron diffraction patterns measured from the same single crystals. This observation offers a simple explanation for the complex magnetic ordering, namely, that it is determined by the enhanced RKKY coupling at the nesting wave vector of the normal-state Fermi surface.

The single crystals for the present study were grown by the floating-zone method from stoichiometric polycrystalline feed rods [19] and cleaved *in situ* perpendicular to the (001) direction immediately before measurement in ultrahigh vacuum of 10^{-10} mbar. For a detailed description of our experimental geometry see Ref. [20]. The measurements were performed within ~24 h after cleavage using 150 eV photons—the excitation energy that was found to yield maximal photocurrent. In the ARPES data presented below, no band replicas that might be indicative of surface reconstruction could be observed, and no aging of the sample surface was detected on the time scale of the experiment, which lets us conclude that the measured band structure is representative of the bulk.

Figure 2 shows several constant-energy cuts and energy-momentum cuts representing electron dispersions in Gd_2PdSi_3, measured at low temperature ($T = 10$ K). Panel (a) shows the Fermi surface, which consists of an electron barrel at the Γ point surrounded by spindle-shaped electron pockets originating from the same band, as sketched by the white lines. Though the Γ barrel is not well distinguishable in panel (a) due to its low intensity, it can be clearly seen in panel (e), which represents a *K*-Γ-*K* energy-momentum cut. The band bottoms of both Γ- and *M*-centered barrels lie at 0.5 eV below the Fermi level, as follows from panels (d) and (e), where similar pointlike intensity blobs can be seen at both Γ and *M* points (b). At yet higher binding energies, the Γ- and *M*-centered features increase again in size, resulting in a fancy trefoil-like structure at 2.5 eV (c).

The Fermi surface of Tb_2PdSi_3, shown in Fig. 3(a), is very similar, though the Γ-centered barrel is much less intense in the photoemission spectra (b). Nevertheless, it can still be recognized in panel (f) of the same figure, which also shows that both electronlike barrels extend down to 0.5 eV binding energy exactly as in the Gd

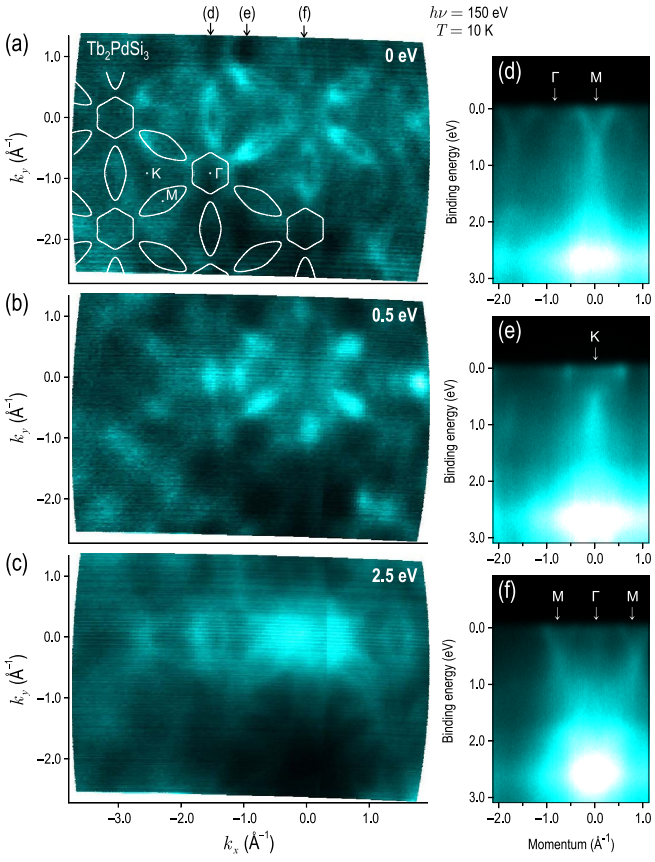

FIG. 3 (color online). Same as Fig. 2, but for Tb_2PdSi_3. Note the similar electronic structure of Gd and Tb compounds near the Fermi level and the differences at higher binding energies, where Tb 4*f* states start to contribute.

compound. At higher binding energies, the electronic structures of the two compounds start to differ (c). Instead of the trefoil-like structure, an intense feature at the Γ point is observed in Tb_2PdSi_3 near 2.5 eV, which can be assigned to the lowest line of the Tb $4f^8 \rightarrow 4f^7$ final state multiplet [17,18,21]. The corresponding $4f^7 \rightarrow 4f^6$ multiplet in Gd is located at higher binding energies and is therefore not observed in our spectra.

Now let us look in more detail at the Fermi surface geometry, as it is shown in Figs. 2 and 3(a), in order to investigate how it affects the momentum-dependent strength of the RKKY coupling and thereby influences the complex magnetic ordering structure that sets in at low temperatures. It is known that in the linear response assumption the coupling constant of the RKKY interaction is determined by the itinerant spin susceptibility of the material (Lindhard function) [15]. From a tight-binding fit to the experimentally measured band structure of R_2PdSi_3, following a procedure similar to that used in Ref. [22], we have calculated the Lindhard function in the static limit ($\omega \rightarrow 0$), which is shown in Figs. 4(a) and 4(b). One sees a strong peak at the $\frac{1}{2}\Gamma K$ wave vector that originates from the perfect nesting of spindle-shaped pockets as sketched in the inset. This peak indicates that the indirect RKKY exchange interaction should be strongly enhanced at the $(\frac{1}{6}\,\frac{1}{6}0)$ wave vector (i.e., halfway from the Γ point towards the corner of the hexagonal Brillouin zone). If one compares this result with the low-temperature neutron diffraction data (Figs. 2 and 3 of Ref. [10]), one sees that the magnetic structure in Tb_2PdSi_3 indeed sets in with the $(\frac{1}{6}\,\frac{1}{6}0)$ in-plane component of the propagation vector.

In Fig. 4(c)–4(f) we show neutron diffraction data obtained from the same single crystals of Tb_2PdSi_3 [23] as our photoemission measurements. Panel (c) shows data in the reciprocal (HHL) plane measured at 11 K, whereas panel (d) shows data in the $(H0L)$ plane. Again, we see a well-defined peak at $H = \frac{1}{6}$ along the (110) direction (Brillouin zone diagonal) already at 11 K, which gets even stronger upon cooling (e), whereas no peaks along (100) direction are observed down to 1.5 K (f). This observation confirms that the low-temperature short-range magnetic ordering of the localized Tb $4f$ electrons is characterized by the $(\frac{1}{6}\,\frac{1}{6}0)$ propagation vector, as dictated by the nesting-driven enhancement of the RKKY interaction at this wave vector. The intense peaks observed at $H = \pm 0.5$ and $H = 0$ in both diffraction patterns originate from the long-range magnetic order predetermined by the crystallographic superstructure, which is driven mainly by the antiferromagnetic exchange interaction along the L direction. The corresponding diffraction reflections are therefore irrelevant to our discussion, since the out-of-plane component is inaccessible in our present ARPES measurements. Our recent neutron diffraction studies (not shown) have revealed magnetic order with the same in-plane propagation vector of $(\frac{1}{6}\,\frac{1}{6}0)$ also in Dy_2PdSi_3 ($T_N = 8.2$ K [12]).

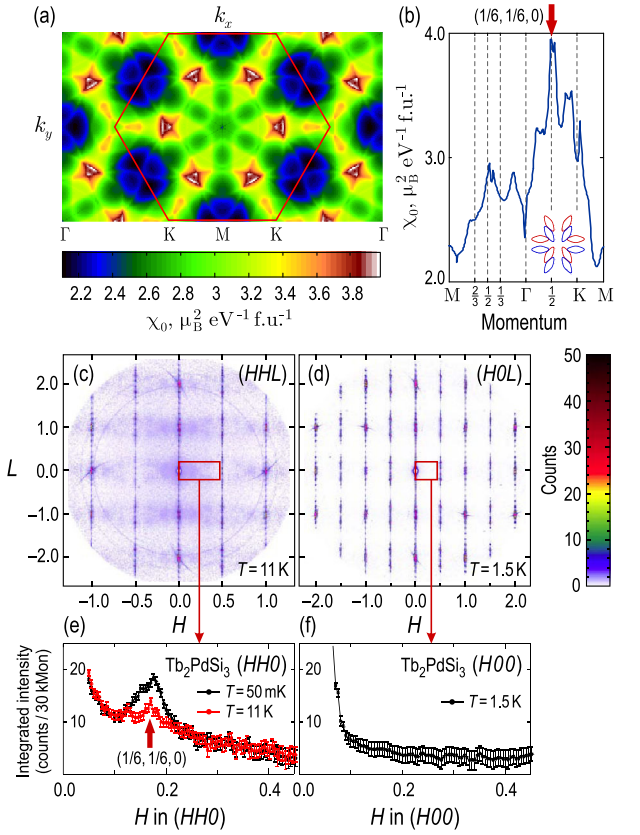

FIG. 4 (color online). Nesting properties of the $Tb(Gd)_2PdSi_3$ Fermi surface. (a) Real part of the Lindhard function at $\omega \rightarrow 0$ as a function of momentum. The hexagon marks the Brillouin zone boundary. (b) Corresponding profile along high-symmetry directions, with the dominant nesting vector marked by the arrow. The same vectors can be seen in panel (a) as white spots. The inset shows the external tangency of the spindle-shaped pockets responsible for the nesting peak at the $\frac{1}{2}\Gamma K$ wave vector. (c) and (d) Neutron diffraction patterns measured from Tb_2PdSi_3 single crystals in the (HHL) and $(H0L)$ planes at 11 and 1.5 K, respectively. (e) and (f) Corresponding intensity profiles along H, integrated within the rectangles shown in panels (c) and (d). The arrow in panel (e) marks that position of the diffraction peak that coincides with the nesting peak in panel (b).

It is appropriate to mention here that magnetic structures with the $(\frac{1}{6}\,\frac{1}{6}0)$ propagation vector were proposed in other rare-earth intermetallics with magnetically frustrated triangular lattices, such as ZrNiAl-type systems, where indirect RKKY exchange also plays a role [24]. This might motivate future studies of the electronic structure in intermetallic compounds. Reference [24] also proposes an explicit arrangement of magnetic moments on a triangular lattice that corresponds to the $(\frac{1}{6}\,\frac{1}{6}0)$ kind of ordering, which might turn out to be relevant for the R_2PdSi_3 systems as well.

To conclude, we have investigated the low-energy electronic structure and Fermi surface geometry of two ternary rare earth silicides that show highest Néel temperatures among the R_2PdSi_3 series of compounds. We have shown

that both compounds possess similar Fermi surfaces with a strong nesting vector that enhances indirect RKKY exchange interaction at the $(\frac{1}{6}\,\frac{1}{6}\,0)$ wave vector, in perfect agreement with the in-plane propagation vector of the low-temperature magnetic ordering observed in our neutron diffraction measurements on the same single crystals. Therefore we conclude that the low-temperature magnetic ordering originates from the RKKY interaction, mediated by itinerant Tb 5*d* electrons at the Fermi level, and is driven by the enhanced itinerant spin susceptibility at the magnetic propagation vector, which can be understood within a simple Fermi surface nesting picture.

This project is part of the Forschergruppe FOR538 and is partially supported by the DFG under Grants No. KN393/4 and BO1912/2-1, as well as DFG research project SFB 463. ARPES experiments were performed using the 1^3-ARPES end station at the UE112-lowE PGMa beam line of the Berliner Elektronenspeicherring-Gesellschaft für Synchrotron Strahlung m.b.H. (BESSY). Authors gratefully acknowledge the scientific and technical support from the team of the E2 diffractometer at Helmholtz-Zentrum Berlin für Materialien und Energie GmbH, where neutron scattering experiments were performed. We are thankful to Fei Tang for a motivating discussion. We also thank R. Hübel, S. Leger, and R. Schönfelder for technical support and N. Wizent for the assistance with sample preparation.

[1] S. R. Saha, H. Sugawara, T. D. Matsuda, Y. Aoki, H. Sato, and E. V. Sampathkumaran, Phys. Rev. B **62**, 425 (2000).
[2] R. Mallik, E. V. Sampathkumaran, M. Strecker, and G. Wortmann, Europhys. Lett. **41**, 315 (1998).
[3] S. R. Saha, H. Sugawara, T. D. Matsuda, H. Sato, R. Mallik, and E. V. Sampathkumaran, Phys. Rev. B **60**, 12162 (1999).
[4] E. V. Sampathkumaran, H. Bitterlich, K. K. Iyer, W. Löser, and G. Behr, Phys. Rev. B **66**, 052409 (2002).
[5] R. Mallik, E. V. Sampathkumaran, and P. L. Paulose, Solid State Commun. **106**, 169 (1998).
[6] A. Szytula, M. Hofmann, B. Penc, M. Slaski, S. Majumdar, E. V. Sampathkumaran, and A. Zygmunt, J. Magn. Magn. Mater. **202**, 365 (1999).
[7] P. L. Paulose, E. V. Sampathkumaran, H. Bitterlich, G. Behr, and W. Löser, Phys. Rev. B **67**, 212401 (2003).
[8] D. X. Li, S. Nimori, Y. Shiokawa, Y. Haga, E. Yamamoto, and Y. Onuki, Phys. Rev. B **68**, 012413 (2003).
[9] S. Majumdar, E. V. Sampathkumaran, P. L. Paulose, H. Bitterlich, W. Löser, and G. Behr, Phys. Rev. B **62**, 14207 (2000).
[10] M. Frontzek, A. Kreyssig, M. Doerr, A. Schneidewind, J.-U. Hoffmann, and M. Loewenhaupt, J. Phys. Condens. Matter **19**, 145276 (2007).
[11] P. A. Kotsanidis, J. K. Yakinthos, and E. Gamari-Seale, J. Magn. Magn. Mater. **87**, 199 (1990).
[12] M. Frontzek, A. Kreyssig, M. Doerr, M. Rotter, G. Behr, W. Löser, I. Mazilu, and M. Loewenhaupt, J. Magn. Magn. Mater. **301**, 398 (2006).
[13] R. Mallik, E. V. Sampathkumaran, P. L. Paulose, H. Sugawara, and H. Sato, Physica (Amsterdam) **B259–B261**, 892 (1999).
[14] R. Mallik and E. V. Sampathkumaran, J. Magn. Magn. Mater. **164**, L13 (1996); E. V. Sampathkumaran, I. Das, R. Rawat, and S. Majumdar, Appl. Phys. Lett. **77**, 418 (2000); S. Majumdar, H. Bitterlich, G. Behr, W. Löser, P. L. Paulose, and E. V. Sampathkumaran, Phys. Rev. B **64**, 012418 (2001); M. Frontzek, A. Kreyssig, M. Doerr, J.-U. Hoffman, D. Hohlwein, H. Bitterlich, G. Behr, and M. Loewenhaupt, Physica (Amsterdam) **B350**, E187 (2004); K. K. Iyer, P. L. Paulose, E. V. Sampathkumaran, M. Frontzek, A. Kreyssig, M. Doerr, M. Loewenhaupt, I. Mazilu, G. Behr, and W. Löser, Physica (Amsterdam) **B355**, 158 (2005).
[15] M. A. Ruderman and C. Kittel, Phys. Rev. **96**, 99 (1954); T. Kasuya, Prog. Theor. Phys. **16**, 45 (1956); K. Yosida, Phys. Rev. **106**, 893 (1957); C. Kittel, in *Solid State Physics*, edited by F. Zeitz, D. Turnbull, and H. Ehreinreich (Academic, New York, 1968), Vol. 22, p. 1; Y. Yafet, Phys. Rev. B **36**, 3948 (1987); J. G. Kim, E. K. Lee, and S. Lee, *ibid.* **54**, 6077 (1996); D. N. Aristov, *ibid.* **55**, 8064 (1997); V. I. Litvinov and V. K. Dugaev, *ibid.* **58**, 3584 (1998).
[16] D. V. Evtushinsky, S. V. Borisenko, A. A. Kordyuk, V. B. Zabolotnyy, D. S. Inosov, B. Büchner, H. Berger, L. Patthey, and R. Follath, Phys. Rev. Lett. **100**, 236402 (2008).
[17] A. N. Chaika, A. M. Ionov, M. Busse, S. L. Molodtsov, S. Majumdar, G. Behr, E. V. Sampathkumaran, W. Schneider, and C. Laubschat, Phys. Rev. B **64**, 125121 (2001);
[18] A. Szytuła, A. Jezierski, and B. Penc, Physica (Amsterdam) **B327**, 171 (2003).
[19] G. Graw, H. Bitterlich, W. Löser, G. Behr, J. Fink, and L. Schultz, J. Alloys Compd. **308**, 193 (2000); G. Behr, W. Löser, D. Souptel, G. Fuchs, I. Mazilu, C. Cao, A. Köhler, L. Schultz, and B. Büchner, J. Cryst. Growth **310**, 2268 (2008).
[20] D. S. Inosov, R. Schuster, A. A. Kordyuk, J. Fink, S. V. Borisenko, V. B. Zabolotnyy, D. V. Evtushinsky, M. Knupfer, B. Büchner, R. Follath, and H. Berger, Phys. Rev. B **77**, 212504 (2008).
[21] F. Gerken, J. Phys. F **13**, 703 (1983).
[22] D. S. Inosov, S. V. Borisenko, I. Eremin, A. A. Kordyuk, V. B. Zabolotnyy, J. Geck, A. Koitzsch, J. Fink, M. Knupfer, B. Büchner, H. Berger, and R. Follath, Phys. Rev. B **75**, 172505 (2007); D. S. Inosov *et al.*, New J. Phys. **10**, 125027 (2008); arXiv:0807.3929.
[23] Neutron diffraction measurements on Gd_2PdSi_3 samples were not possible because of large absorption. On the other hand, measurements by x-ray resonant magnetic scattering proved not sensitive enough to detect a possible weak signal from the low-temperature short-range magnetic order in the (110) direction. Preliminary information about magnetic propagation vector in this material can be found in A. Kreyssig, J.-W. Kim, L. Tan, D. Wermeille, A. I. Goldman, M. Frontzek, and M. Löwenhaupt, http://meetings.aps.org/link/BAPS.2005.MAR.U9.10.
[24] Ł. Gondek and A. Szytuła, J. Alloys Compd. **442**, 111 (2007).